International Journal of Thermophysics, Vol. 25, No. 3, May 2004 (© 2004)

Two-Wire Solution for Measurement of the Thermal Conductivity and Specific Heat Capacity of Liquids: Experimental Design

V. Giaretto[1–3] and M. F. Torchio[1]

Received April 29, 2003

After a brief review of the hot-wire method, the design of an experiment that employs a two-wire technique is proposed. Several uncertainty sources are considered in order to define the optimal experimental conditions and evaluate the advantages of the two-wire technique. Convection and radiation effects and finite properties of the wires are discussed. The measurement uncertainties of the temperature rise, the heat flux generated by the hot wire, the time of the measurements, and the radial position of the second wire are considered. The influence of the uncertainty sources on the simultaneous estimation of thermal conductivity and specific heat capacity is analyzed for the hot-wire and two-wire techniques.

KEY WORDS: hot-wire method; specific heat capacity; thermal conductivity; two-wire method; uncertainty analysis.

1. INTRODUCTION

The measurement of the thermal conductivity and specific heat capacity or thermal diffusivity using the hot-wire method has been attempted by many investigators. This transient method has numerous positive characteristics, namely:

- it allows an easy analytical solution [1], in particular, when the heat source is constant;

[1] Dipartimento di Energetica, Politecnico di Torino, C.so Duca degli Abruzzi, 24, 10129 Torino, Italy.
[2] Istituto Nazionale per la Fisica della Materia, C.so Duca degli Abruzzi, 24, 10129 Torino, Italy.
[3] To whom correspondence should be addressed. E-mail: valter.giaretto@polito.it

0195-928X/04/0500-0679/0

- it requires a short measurement time (a few seconds);
- the experimental setup can be simple and inexpensive if limited accuracy is sufficient (it could be useful for *in situ* measurements);
- its accuracy can be improved using suitable corrections [2–6];
- thermal conductivity and specific heat capacity can be measured simultaneously;
- it has proved reliable to measure the thermal properties of gases, [3, 7–11], liquids [5–6, 12–24], solids [25–29], and powders [30, 31];
- it has proved reliable to measure the thermal properties over a wide range of temperatures and pressures [8–10].

Most authors start from a well-known analytical solution [1] and design or improve some components of a pre-existing facility [9]. Other authors propose corrections to the classical analytical solution [2,4]. In other cases, the authors start from a well-known calibrated apparatus and measure the thermal property of new materials (such as a refrigerant [18], lubricant [32], resin [26]) or extend the temperature or pressure range for known materials [7, 8].

In this work, the authors propose the design of an experiment that employs two wires: the hot wire and a second wire positioned near the first one. The hot wire is used both to generate the heat flux in the medium and as a resistance thermometer. The second wire is used only as a resistance thermometer. The two temperature sensor approach has already been considered [33], but the second sensor was usually a thermocouple or a thermistor. The aim of this study is to improve the simultaneous estimation of thermal conductivity and specific heat capacity by using two wires as temperature sensors instead of only one.

Several uncertainty sources have been considered to define the useful experimental conditions and to evaluate the advantages of the two-wire technique for the estimation of the previously mentioned properties. To obtain a general result that is valid for any fluid, a dimensionless approach has been adopted.

Uncertainties due to axial conduction, convection and radiation are discussed. In order to avoid the onset of free convection during the experiments, an appropriate criterion was adopted to establish the measurement zone along the wire.

The line-source analytical model is normally used in the hot-wire method [33]. This model is appropriate when the hot wire is thin, while in other cases the finite properties of the hot wire can introduce a bias to the measurements. The influence of the finite diameter of the hot wire has therefore been considered. The presence of a second wire could produce a deviation in the measurements compared to the case where only

the hot wire is present. In order to verify and quantify this occurrence, the alteration of the thermal field due to the presence of the second wire was studied using a numerical solution (finite element method—FEM). Furthermore, considering the relative uncertainties of the measurements (such as temperature rise, heat flux generated by the hot wire, radial position of the second wire, etc.), an extensive error analysis was carried out and the relative uncertainty of the estimated properties was evaluated. This analysis was useful to set-up the two-wire experimental apparatus.

2. ANALYTICAL MODELS

Usually the employed model refers to the hot-wire method with a continuous line source with a constant heat rate generated per unit time and length in a fluid whose properties are assumed to be temperature independent [1]. To obtain a constant heat rate per unit time, during the experiment it is necessary to control the supplied current appropriately according to the changes in the circuit resistance. In this case, for wires without coatings, when no contact resistance between the wire and the surrounding fluid is considered, the model refers to the following dimensionless equation:

$$\vartheta = \Delta T \frac{\lambda}{q_0} = -\frac{1}{4\pi} Ei\left(-\frac{\xi^2}{4\tau}\right), \tag{1}$$

where both τ and ξ refer to the hot-wire radius, and are the Fourier number and the dimensionless radial position in the fluid, respectively. ϑ is the dimensionless temperature increment defined from the temperature increment ΔT, through the ratio between the thermal conductivity λ of the fluid and the constant heat rate per unit time and per unit length q_0 generated from the hot wire. $Ei(-)$ represents the exponential integral.

If the control of the supply current is avoided during the experiment, the heat rate per unit time generated from the hot wire is not constant. In this way, the apparatus is simpler, but a more general model must be used [1]. The instantaneous value of the heat rate per unit time and per unit length can be defined as the product between the initial constant value q_0 at $\tau = 0$ and a time dependent function $\psi\ (\tau)$, which assumes a unitary value at $\tau = 0$. In this case, the dimensionless temperature ϑ is obtained from the solution of the following integral:

$$\vartheta = \frac{1}{4\pi} \int_0^{\tau} \psi(\tau) \exp\left[-\frac{\xi^2}{4(\tau - \tau')}\right] \frac{d\tau'}{\tau - \tau'}. \tag{2}$$

The models introduced by Eqs. (1) and (2) assume the hot wire is a perfect heat conductor with negligible heat capacity. When the hot wire is very

thin, this hypothesis is appropriate. If the wire dimension is increased, this assumption may no longer be suitable. The wire may still be considered as a perfect heat conductor but the influence of its heat capacity must be taken into account [34]. In this condition, the analytical model is more complicated and the dimensionless temperature ϑ is calculated from the solution of the following improper integral:

$$\vartheta = \frac{2}{\pi^2}\delta \int_0^{\infty} \left[1 - \exp\left(-\tau \nu^2\right)\right] \Theta(\xi, \delta, \nu) d\nu, \tag{3}$$

where δ is the ratio between the specific heat capacity of the fluid and the specific heat capacity of the wire and υ represents an arbitrary variable defined between the lower and upper integration limits. The term Θ is given by the following equation, where J_k(-) and $Y_k(-)$ are the well-known Bessel functions of integer order k:

$$\Theta(\xi, \delta, \upsilon) = \frac{J_0(\xi\upsilon)\left[\upsilon Y_0(\upsilon) - 2\delta Y_1(\upsilon)\right] - Y_0(\xi\upsilon)\left[\upsilon J_0(\upsilon) - 2\delta J_1(\upsilon)\right]}{\upsilon^2\left\{\left[\upsilon Y_0(\upsilon) - 2\delta Y_1(\upsilon)\right]^2 + \left[\upsilon J_0(\upsilon) - 2\delta J_1(\upsilon)\right]^2\right\}}. \tag{4}$$

An accurate solution of the previous integrals can be found using the Romberg integration with successive refinements [35], also when the integral is improper, using an open formula. In order to obtain suitable values of the Bessel functions, their approximation can be made with high accuracy coefficients [36].

3. UNCERTAINTY SOURCES

3.1. Influence of Axial Conduction, Free Convection and Radiation

As far as axial conduction is concerned, Haarman [2] studied the influence of the finite length of the wire computing the average value of the temperature rise by integrating over the length of the wire. For an assigned wire length and diameter, if the wire ends are kept at a constant temperature, depending on the fluid and wire properties, the axial flow can introduce a significant deviation to the temperature rise (several percent) with respect to the pure radial flow assumption (wire infinitely long). For analogous conditions, in previous work Blackwell [37] studied the error caused by assuming a pure radial flow, but he calculated the deviation of the temperature rise in the center of the wire. Assuming a criterion in terms of a length/radius, and choosing an appropriate dimensional ratio (e.g., length 50 times the radius), he demonstrated how the deviation from the ideal temperature rise becomes negligible in the center

of the wire length. Subsequently, Blackwell [38] analyzed the influence of axial heat loss in the calculation of the thermal conductivity for an infinitely long wire, but which is heated for only a finite length. Without contact resistance between the wire and the fluid, the relative error of thermal conductivity λ of the fluid is a function of the wire and fluid properties and the Fourier number τ,

$$\frac{\Delta\lambda}{\lambda} = \pi^{1/2} e^{\frac{-\gamma^2}{4\tau}} \left[\frac{(4\tau)^{1/2}}{\gamma} + 2\gamma \left(\mu - \delta^{-1}\right) (\ln 4\tau - G)\,(4\tau)^{-3/2} \right], \qquad (5)$$

where γ is the ratio of the length to radius of the wire, μ is the ratio of the thermal conductivity of the wire to that of the fluid, δ is the ratio of the heat capacity per unit volume of the fluid to that of the wire, and G is the Euler constant. As an example, for μ values that range between 120 and 450, and δ values that range between 0.5 and 1.5, at a τ value of 1000, a minimum γ value of 180 is required to obtain a relative error of thermal conductivity of less than 0.5%. Therefore, if the potential leads are positioned along the wire not too close to the ends, without compensation, the axial flow can be neglected by choosing an appropriate value of the ratio γ.

The hot-wire technique is based on the assumption that the heat transfer within the fluid is only controlled by heat conduction, but it is known that convective currents in fluids can introduce errors in the results. In the hot-wire method, an estimable time period exists (measured from the beginning of the heating process) in which the convection effect is negligible. This way, if the measurement cycle is completed before the end of this period, convection effects can be neglected. Both experimental and analytical techniques are employed to estimate this time. If a constant heat rate per unit time is applied, when the Fourier number is much greater than one, and other heat losses do not start earlier (i.e. radiation), the onset of free convection can be detected experimentally. In this case, if the temperature rise of the hot wire is plotted vs. time, the free convection starts when the plot deviates from a straight line. Kawaguci et al. [23] suggested an algorithm for the detection of natural convection in an automated apparatus. Analytical or experimental studies are necessary to systematically understand the characteristics of the convection effects. Goldstein and Briggs [39] studied transient free convection with semi-infinite vertical cylinders, from an analytical point of view, introducing a geometrical parameter ζ, called the dimensionless convection penetration distance, defined as

$$\zeta = z \frac{\lambda}{g\beta q_0 t^2}, \qquad (6)$$

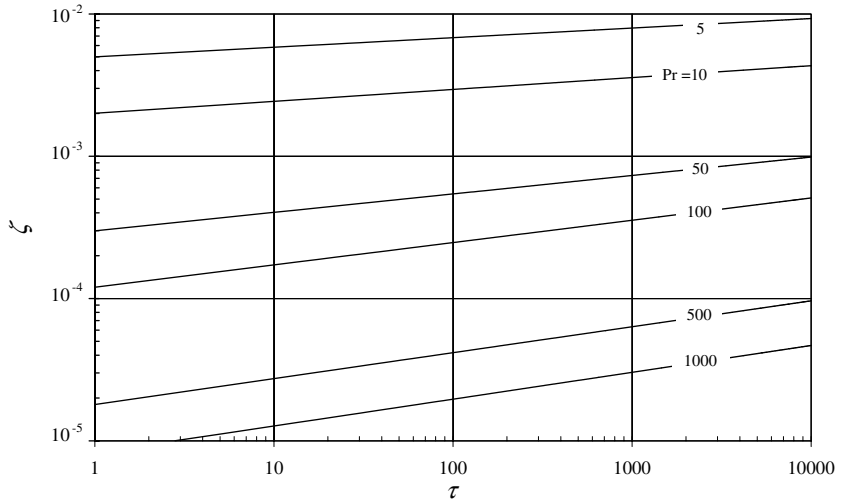

Fig. 1. Dimensionless penetration distance ζ from the leading edge of the free convection of a semi-infinite cylinder vs. the Fourier number τ,for a few Prandtl numbers.

where z is the convection penetration distance from the leading edge, λ is the thermal conductivity of the fluid, g is the acceleration of gravity, β is the isobaric thermal expansion coefficient, q_0 is the constant heat generation per unit time and per unit length in the wire, and t is the time.

The solutions for the dimensionless penetration distance ζ vs. the Fourier number are shown in Fig. 1 for a few Prandtl numbers. For a given fluid, fixing q_0, the lower penetration distance z vs. time could be obtained. On the contrary, if the maximum penetration distance is imposed by the geometrical characteristics of the apparatus, the maximum duration of an experiment can be defined to avoid convection in the measurement zone from the lower edge. Since the length of the wire is finite, another penetration distance from the upper edge must be considered. Saito et al. [14] showed that the upper penetration distance is smaller than the lower one. Therefore, the measurements must be performed in the gap between the lower and upper penetration distances; as a precaution, the upper distance could be assumed equal to the lower one. For an assigned fluid, if a maximum theoretical duration of the experiment is assumed, and Eq. (6) is used, the calculated distance z from the leading edge allows the position of the potential leads along the wire to be defined.

An amount of the thermal energy is transferred from the hot wire by radiation through the fluid; this consequently reduces the conducted heat. In this case, the apparent thermal conductivity becomes higher than

the real value. When the fluid does not contribute directly or indirectly to radiation through absorption and emission, the problem can be solved by considering a transparent fluid bounded by grey surfaces. Concerning liquids Nieto de Castro et al. [5] concluded that, in view of the small temperature rises involved in their measurements (5–10°C), the radiation effect is expected to be no more than 1% of the thermal conductivity. The effects of radiation become more pronounced for stronger absorbing liquids and for large temperature increases.

To consider the contribution of radiation to the measurements, Nieto de Castro et al. [40], and more recently Sun et al. [41] who took the properties of the wire into account, corrected the temperature rise by assuming a perfect diffusive radiation model. The heat loss due to radiation depends in particular on both the thermal and optical properties of the fluid, and it increases in time. If the corrections introduced by Sun et al. [41] are considered, for an uncoated wire, the relative deviation of the temperature rise, with respect to the ideal line-source solution, can be expressed as

$$\frac{\Delta T' - \Delta T}{\Delta T'} = -4D\left[\frac{2}{\delta} + \ln 4\tau - G - \frac{\pi^2/6 + 4\tau + 2}{\ln 4\tau - G}\right], \tag{7}$$

where $\Delta T'$ and ΔT are the ideal and the measured temperature rises, respectively, and G is the Euler constant. The coefficient D is defined as

$$D = \frac{Kn^2\sigma T_0^3}{\lambda} r_{\mathrm{HW}}^2, \tag{8}$$

where K is the mean absorption coefficient, n is the refractive index, σ is the Stefan–Boltzmann constant, λ is the thermal conductivity of the fluid, r_{HW} is the hot-wire radius, and T_0 is the initial cell temperature. If a suitable set of values is chosen for these quantities (e.g., $5 \leqslant r_{\mathrm{HW}} \leqslant 50\,\mu$m, $0.1 \leqslant \lambda \leqslant 1\,\mathrm{W{\cdot}m^{-1}{\cdot}K^{-1}}$, $100 \leqslant Kn^2 \leqslant 1000\,\mathrm{m^{-1}}$, and $300 \leqslant T_0 \leqslant 500\,\mathrm{K}$), the order of magnitude of coefficient D can be assumed to be from 10^{-7} to 10^{-5}. Moreover, according to Eq. (7), the relative temperature deviation depends on the ratio δ and the Fourier number τ. As an example, for δ values that range between 0.5 and 1.5, when the coefficient D is 10^{-7}, the temperature deviation is negligible up to a τ value of 1000, whereas, for a D value of 10^{-5}, the relative temperature deviation is less than 0.5% for a τ value of less than 200, and becomes 2% at a τ value of 1000. The radiation effect on the measured temperature rise induces a deviation from the ideal straight line that is similar to the convection effect, but its contribution could produce evident effects before convection does. Therefore, the ideal line-source solution can be used without

radiation correction, if an appropriate maximum experiment duration is adopted.

The hot wire length and radius, the position of the potential leads, and the maximum experimental duration are related. Depending on the fluid properties and test conditions (i.e., the initial cell temperature T_0 and the generated heat flux q_0), if the hot wire characteristics (material, length, and radius) are chosen, the position of the potential leads and the maximum experiment duration could be fixed to limit the influence of the axial conduction, convection, and radiation heat losses.

3.2. Influence of the Heat Capacity of the Hot Wire

In many cases, very thin wires are used (5–10 μm diameter) and the line source approximation of Eq. (1) gives suitable solutions. However, in engineering applications, the diameter of the hot wire must be large enough for durable use. In this case, the line source approximation can introduce a significant bias. As previously mentioned, the large diameter of a hot wire could require the use of a model like Eq. (3), where its heat capacity is taken into account. In order to obtain a suitable and stable solution, Eq. (3) requires more computation time than Eq. (1), especially when numerical derivatives and nonlinear regressions are performed on experimental data to estimate the properties of the fluid.

An analytical study was carried out to try to understand when the wire heat capacity must be taken into account. The influence of the radial dimension of the hot wire was studied using a constant heat flow rate per unit time and unit length, comparing the dimensionless temperature ϑ obtained by Eqs. (1) and (3). The absolute values of the dimensionless temperature deviation $\Delta\vartheta$ of the two models were calculated vs. the Fourier number τ, for several dimensionless positions ξ in the fluid, using a few different values of the parameter δ (ratio between the specific heat capacity of the fluid and the wire). Usually the wire is made of platinum and typical reference mediums are liquids like toluene or water. Near ambient temperature, the ratio δ is close to 0.5 for toluene and 1.5 for water; otherwise, at the same temperatures, δ is close to 1.0 for liquids like glycerin or propylene glycol. These three values of δ were adopted, as well as several values of ξ ranging between 1 and 100 ($\xi = 1$ is the position that corresponds to the hot-wire radius).

At the beginning of the transient process, the absolute value of the deviation $\Delta\vartheta$ increases and reaches its maximum for different τ values, according to the position of ξ. The maximum values of the absolute deviations $\Delta\vartheta$ vs. the dimensionless position ξ are shown in Fig. 2. These values are higher close to the hot-wire radius and decrease quite rapidly

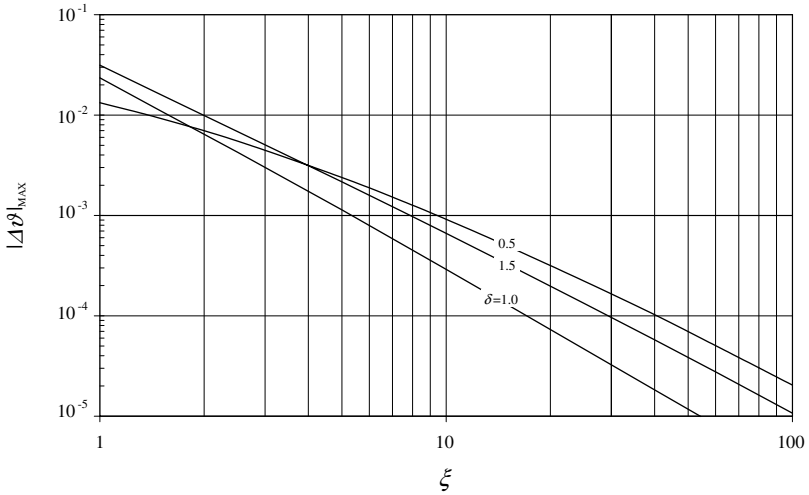

Fig. 2. Absolute value of the maximum dimensionless temperature deviation $\Delta\vartheta$ vs. the dimensionless position ξ in the fluid. A comparison between the solution obtained from Eq. (1), the line source, and Eq. (3), the finite diameter of the hot wire; δ is the ratio between the specific heat capacity of the fluid and the wire.

when the dimensionless position ξ increases, whatever δ value is adopted. When the specific heat capacity of the fluid is greater than the specific heat capacity of the wire, $\delta>1$, $\Delta\vartheta$ vs. ξ decreases more rapidly than the opposite case when $\delta<1$. Furthermore, we can observe from this figure, how the same specific heat capacity of the wire and the fluid ($\delta=1$) do not produce null values of $\Delta\vartheta$. This occurs because the thermal conductivity of the wire is finite, and is usually much higher than the thermal conductivity of the fluid, while the model of Eq. (3) assumes that the wire is a perfect heat conductor.

The values of $\Delta\vartheta$ at the positions $\xi=1$ and $\xi=15$ vs. the Fourier number τ are shown in Fig. 3 for the three adopted values of parameter δ. When $\xi=1$ (as is the case of the single-wire technique), and δ is near to one or even greater, $\Delta\vartheta$ reaches its maximum for τ values of less than one. When δ is less than one, the maximum of $\Delta\vartheta$ occurs for values of τ between 1 and 10. Greater values of ξ translate the maximum $\Delta\vartheta$ toward greater values of τ; for the case shown in the figure, $\xi=15$, the maximum values of $\Delta\vartheta$ are positioned between 50 and 100τ.

When a line source approximation is used with a large wire, an appropriate delay time from the start of the transient must be adopted before collecting suitable measurements to avoid the influence of the hot-wire heat capacity. Depending on the fluid, this delay should not be too long to avoid convection and radiation. Therefore, during the experiment an

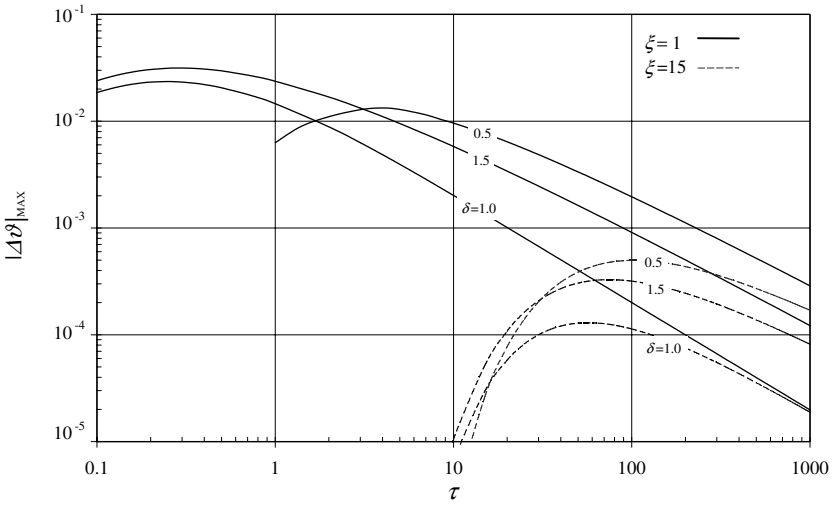

Fig. 3. Absolute value of the maximum dimensionless temperature deviation $\Delta\vartheta$ vs. the Fourier number τ, in the $\xi = 1$ (hot-wire radius) and $\xi = 15$ positions. A comparison between the solution obtained from Eq. (1), the line source, and Eq. (3), the finite diameter of the hot wire; δ is the ratio between the specific heat capacity of the fluid and the wire.

appropriate time interval can be found where the influences of both the heat capacity of the hot wire, convection and radiation are negligible. Finally, it is possible to affirm that the influence of the heat capacity of the hot wire is evident only in the zone surrounding the wire. After a distance from the hot wire axis that corresponds to 15 times its radius ($\xi = 15$), the influence of the heat capacity of the hot wire decreases by about of two orders of magnitude and becomes insignificant at a distance of thirty times its radius.

3.3. Influence of the Second Wire

As previously mentioned, a second wire is employed to evaluate the advantages of the estimation of the thermal conductivity and the specific heat capacity of the fluid. The second wire is used only as a resistance thermometer. In this section, we consider whether the presence of the second wire can disturb the measurement significantly. The presence of the second wire introduces both a nonhomogeneous material and a local heat generation due to its feed current into the fluid. Let us consider only a radial temperature gradient in an infinite medium. Assuming

the properties of the fluid and the wires as temperature independent, the following dimensionless equation was adopted:

$$\frac{d^2\vartheta}{d\eta^2}+\frac{1}{\eta}\frac{d\vartheta}{d\eta}+\varphi=\frac{d\vartheta}{d\tau^*}, \tag{9}$$

where ϑ represents the previous defined dimensionless temperature increment, η is the dimensionless position in the fluid defined as the ratio between the radial position and the radius of the second wire, τ^* is the Fourier number referring to the second-wire radius and the fluid diffusivity, and $\varphi=\varepsilon^2/\pi$ represents the dimensionless heat generation, where ε is the ratio between the radius of the second wire and the hot wire ($\eta=\varepsilon\xi$). Equation (9) was solved numerically in the radial domain using the finite element method, with the nonuniform meshing criteria shown in Fig. 4. Only the part of the studied domain near the wires is represented in this figure. More than 30,000 triangular elements and more than 15,000 nodes were used, and semi-infinite elements were also applied to the boundary in order to consider the specific unbounded field problem. Three different values of the parameter ε were assumed (1, 0.5, and 0.25) and several different positions of the second wire in the fluid (η), ranging between 10 and 200, were considered. A dimensionless heat generation was uniformly applied to the wire elements, using a value of φ a thousand times lower than the heat generation on the hot wire for the second wire. The

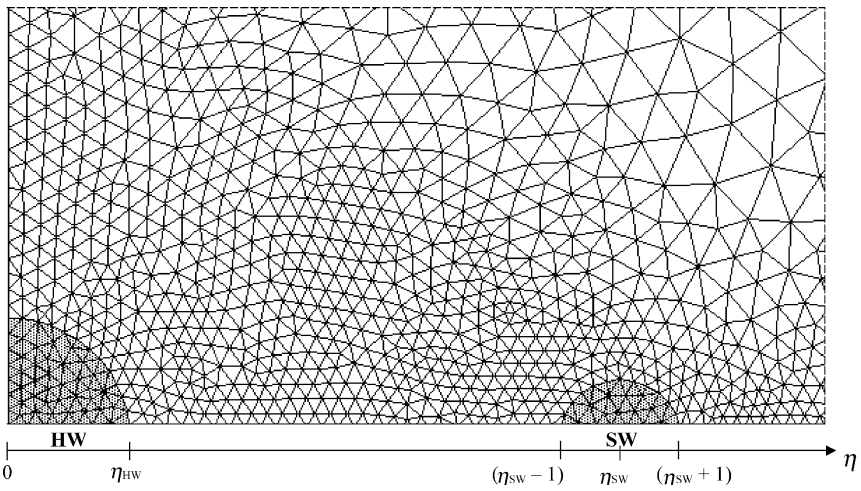

Fig. 4. Part of the mesh near the wires for the FEM analysis. The complete mesh includes 30,126 triangular elements and 15,434 nodes. η is the dimensionless position in the fluid that refers to the second-wire radius.

dimensionless properties of the fluid were assumed to be unitary, whereas the properties of the wires were referred to the fluid ones. In this analysis, an average dimensionless temperature ϑ was calculated for each wire as the average value of the dimensionless temperature of its nodes.

Two dimensionless temperature deviations $\Delta\vartheta$ vs. the Fourier number τ^* were calculated: on the hot wire and on the second wire positions. The deviation $\Delta\vartheta$ was obtained by comparing the results when the second wire was present or when it was not present. Moreover, several positions of the second wire in the fluid were considered.

The maximum values of $\Delta\vartheta$, calculated on the two wires vs. the dimensionless position η in the fluid of the second wire, are shown in Fig. 5. In this figure, the maximum deviation takes place when the second wire is close to the hot one. The maximum deviation $\Delta\vartheta$ is practically independent of the dimensionless properties of the wires and of the considered values of parameter ε, and depends only on the position of the second wire in the fluid. Different values and trends of $\Delta\vartheta$ were found for the two wires. For the hot wire, with respect to the second one, $\Delta\vartheta$ is higher for values of η that are lower than 60 and tends to be significantly reduced when η increases. On the contrary, due to heat generation, the deviation $\Delta\vartheta$ for the second wire tends to a constant value for η that

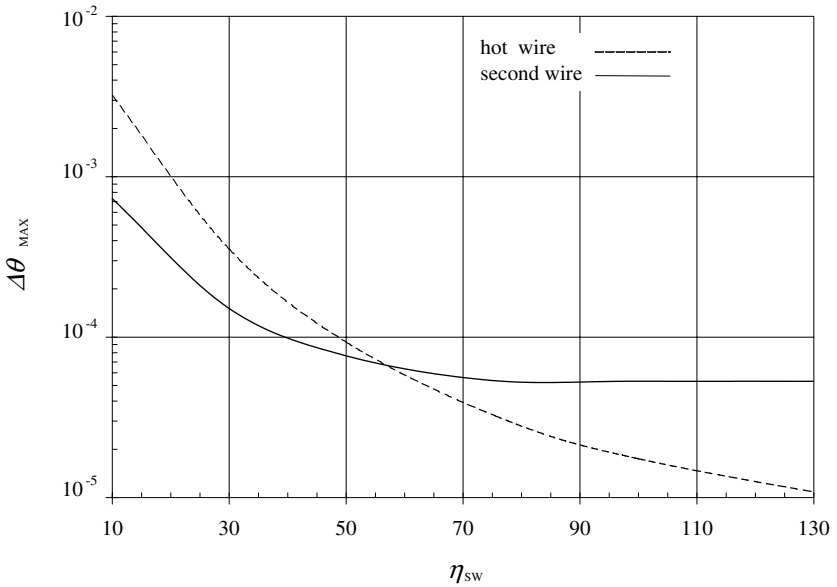

Fig. 5. Maximum dimensionless temperature deviation $\Delta\vartheta$ vs. position η_{SW} of the second wire in the fluid. The influence of the presence of the second wire on the hot-wire measurements (dashed line) and by itself (continuous line).

is greater than 80. In short, the influence of the second wire is negligible when it is not very close to the hot wire ($\eta > 40$).

4. UNCERTAINTY OF THE ESTIMATED PROPERTIES

In the previous sections, the influences of the finite diameter of the hot wire and of a second wire were analyzed when a two-wire technique was used. The calculated temperature deviation in these cases causes an uncertainty induced by the model on the estimated properties, which is not dependent on the experimental measurements. The uncertainties on the temperature and on the generated heat flux are calculated from the estimated standard uncertainties of each measured quantity. Furthermore, if the uncertainty of the time measurement related to the whole experiment duration, and the uncertainty of the second wire position (when one is used) are considered, we can define the variance u_ϑ^2 of the dimensionless temperature ϑ as the combined variance of the considered single uncertainty source with the equation:

$$u_\vartheta^2 = u_{\vartheta,HW}^2 + u_{\vartheta,SW}^2 + u_{\vartheta,\Delta T}^2 + u_{\vartheta,q_0}^2 + u_{\vartheta,\tau}^2 + u_{\vartheta,\xi}^2, \tag{10}$$

where $u_{\vartheta,\mathrm{HW}}$ and $u_{\vartheta,\mathrm{SW}}$ are the dimensionless standard uncertainties associated with the dimensionless temperature deviation due to the heat capacity of the hot wire and the second wire, respectively, $u_{\vartheta,\Delta T}$ and u_{ϑ,q_0} are the dimensionless standard uncertainties induced on ϑ by the measurement uncertainty of ΔT and q_0, while $u_{\vartheta,\tau}$ represents the dimensionless standard uncertainty of the Fourier number associated to the measurement uncertainty of time t and $u_{\vartheta,\xi}$ is the dimensionless standard uncertainty related to the position of the second wire, when present. Considering Eq. (1), and the definitions of ϑ, ξ and τ, the last four components of uncertainty in Eq. (10) can be expressed as follows:

$$u_\vartheta^2 = u_{\vartheta,HW}^2 + u_{\vartheta,SW}^2 + \vartheta^2 \left[\left[\frac{u_{\Delta T}}{\Delta T} \right]^2 + \left[\frac{u_{q_0}}{q_0} \right]^2 \right] + \\ + \left[\frac{\partial \vartheta}{\partial \tau} \right]^2 \tau^2 \left[\frac{u_t}{t} \right]^2 + \left[\frac{\partial \vartheta}{\partial \xi} \right]^2 \xi^2 \left[\frac{u_r}{r} \right]^2. \tag{11}$$

The terms $u_{\Delta T}/\Delta T$ and u_{q0}/q_0 are the relative measurement uncertainties of the temperature rise and the heat flux per unit length generated from the hot wire, respectively. The quantity u_t/t represents the relative uncertainty of the time position of the measurements, and u_r/r is the relative uncertainty of the radial position of the second wire, when used.

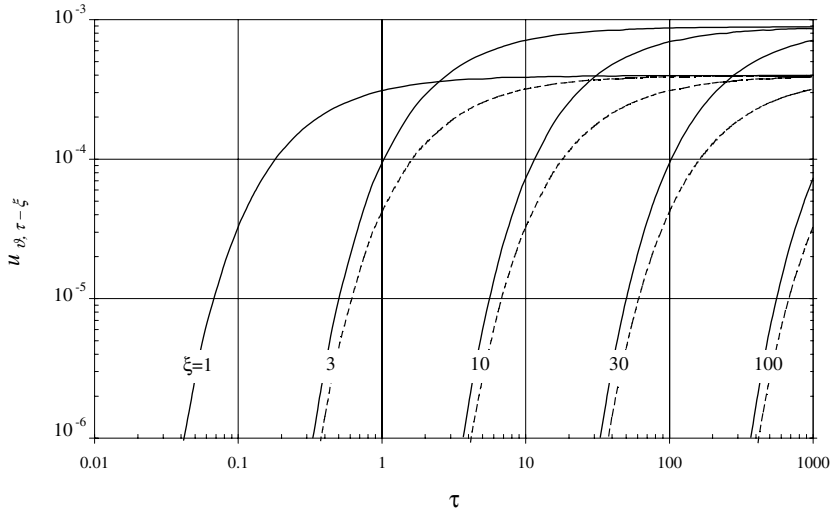

Fig. 6. Standard uncertainty of the dimensionless temperature ϑ vs. the Fourier number τ, induced by the relative uncertainty of the time position of the measurements and the relative uncertainty of the second wire position in the fluid, for a few different ξ values. $\xi = 1$, hot-wire radius, where only the time uncertainty is present. For the other ξ values: the uncertainty of the time position, dashed lines, the uncertainties of the time position and second wire position, continuous lines.

The last two terms of Eq. (11), the variances $u^2_{\vartheta,\tau}$ and $u^2_{\vartheta,\xi}$, contain the partial derivatives of the function ϑ with respect to the Fourier number τ and the dimensionless position ξ. These derivatives were calculated numerically assuming the model of Eq. (1). The combined standard uncertainty $u_{\vartheta,\tau-\xi}$, calculated as the positive square root of the combined variances $u^2_{\vartheta,\tau}$ and $u^2_{\vartheta,\xi}$, is plotted in Fig. 6, vs. the Fourier number τ for a few values of ξ, assuming $u_t/t = u_r/r = 0.5\%$. For the position $\xi = 1$ (hot-wire radius) only the uncertainty of time t is present. For the other ξ positions, the effects of both uncertainties are present; the dashed lines represent the contribution of the uncertainty to time t and the continuous lines combine the two effects. With the same relative uncertainty of t and r, the influence on ϑ of the uncertainty position of the second wire is about two times the effect induced by the uncertainty of time t. The maximum value of $u_{\vartheta,\tau-\xi}$ tends to a constant value, which occurs at increasing τ values, depending on the position (ξ).

The value assumed from Fig. 2 for $u_{\vartheta,\mathrm{HW}}$ corresponds to the maximum deviation $\Delta\vartheta$ for $\xi = 1$ and $\delta = 1.5$. If the dimensionless position $\xi = 30$ ($\eta = 45$) for the second wire is chosen, the value of $u_{\vartheta,\mathrm{SW}}$ from Fig. 5 is assumed to be equal to 0.0001 for both wires. The combined standard relative uncertainty u_ϑ/ϑ for the hot wire and the second wire at

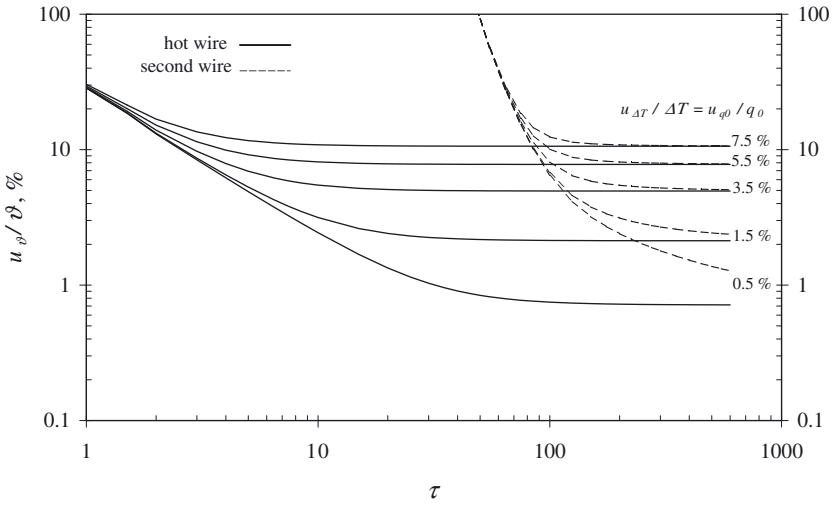

Fig. 7. Relative standard uncertainty of the dimensionless temperature ϑ vs. the Fourier number τ, induced by all the uncertainty (both experimental and those of the model), for the different relative uncertainties of the temperature rise. The relative uncertainty of the constant heat flux per unit length is assumed to be equal to the relative uncertainty of the temperature rise.

the position $\xi = 30$ is plotted in Fig. 7 vs. the Fourier number, as an example. These relative uncertainties were calculated for several values of the measurement uncertainty that ranged between 0.5% and 7.5%, assuming $u_{\Delta T}/\Delta T = u_{q_0}/q_0$. For the hot wire it can be seen that u_ϑ/ϑ is high and practically independent of the measurement uncertainties for small values of the Fourier number τ. At the beginning of the transient, the influence of the hot wire heat capacity is prevalent with respect to other uncertainty sources. The relative uncertainty decreases when the Fourier number increases and becomes constant after $\tau = 100$ for each case. A similar behavior was found for the second wire, but u_ϑ/ϑ is very high for τ values of less than 100, where ϑ is negligible. For greater τ values, the relative uncertainty is quite similar to the previous case, but it is always greater than the hot wire u_ϑ/ϑ.

The model of Eq. (1) was adopted to evaluate the uncertainty of the estimated properties. Equation (1) can be written in dimensional form, introducing the measurement error $\Delta_{\Delta T}$ and the properties λ' and C', which represent the best estimate of the correct λ and C:

$$\Delta T' = -\frac{q_0}{4\pi \cdot \lambda'} Ei\left[-\left(\frac{r}{r_{\mathrm{HW}}}\right)^2 \left(4\frac{\lambda'}{C'}\frac{t}{r_{\mathrm{HW}}^2}\right)^{-1}\right], \tag{12}$$

where $\Delta T' = \Delta T + \Delta_{\Delta T}$, $\lambda' = \lambda + \Delta\lambda = \Lambda\lambda$, and $C' = C + \Delta C = \chi C$.

Equation (12) can again be written in dimensionless form, introducing the parameters Λ and χ which were previously defined as the ratio between the estimated properties and their correct value:

$$\vartheta' = \vartheta + \Delta\vartheta = \frac{\Delta T' \lambda'}{q_0} = -\frac{1}{4\pi\Lambda} Ei\left[-\frac{\xi^2}{4\tau\Lambda/\chi}\right]. \tag{13}$$

The quantity $\Delta\vartheta$ is the dimensionless error of ϑ that includes the overall experimental uncertainty; $\Delta\vartheta$ was assumed to be equal to $\pm 3u_\vartheta$.

The relative errors of the thermal conductivity and specific heat capacity are therefore calculated, respectively, as $1-\Lambda$ and $1-\chi$. When Λ and χ are unitary, $\lambda' = \lambda$ and $C' = C$, there are no measurement errors ($\Delta_{\Delta T} = 0$) and $\vartheta' = \vartheta$. The dimensionless temperature ϑ' was calculated using several values of the measurement uncertainty $u_{\Delta T}/\Delta T$ and u_{q_0}/q_0 ranging between 0.5 and 7.5%. The parameters Λ and χ were simultaneously estimated [43] using the model of Eq. (1), by nonlinear regression on ϑ', both considering only the hot wire and the hot wire and second wire together. A maximum likelihood estimator (ML) was adopted [44] to estimate these parameters. Like other estimators (i.e., weighted least squares), ML uses the sensitivity matrix to estimate the unknown parameters. The sensitivity matrix contains the first derivatives of the dependent variable with respect to the parameters. For multi-response experiments (i.e., the temperatures measured by the hot wire and the second wire), the sensitivity matrix and the covariance matrix of the measurement uncertainties play an important role in assigning an appropriate weight to each temperature sensor. The sensitivity coefficients are time and position dependent, so that each temperature sensor assumes a different influence on the estimating values. The hot wire response is usually essential in the first part of the useful transient where the second wire response is negligible, while the second wire response becomes more important in the last part of the experiment.

Since the two sensors provide different responses, the reference temperature that has to be assigned to the estimated properties can be assumed as a linear combination of the average temperature variations measured by the two sensors. In the experiment duration $t - t_0$, the reference temperature T_{ref} can be determined as

$$T_{\text{ref}} = T_0 + \left[\frac{1-\omega}{t-t_0}\int_{t_0}^{t} \Delta T_{\text{HW}}(t')dt' + \frac{\omega}{t-t_0}\int_{t_0}^{t} \Delta T_{\text{SW}}(t')dt'\right], \tag{14}$$

where ω is a weight coefficient defined as

$$\omega = \frac{\int_{t_0}^{t} \Delta T_{SW}(t')dt'}{\int_{t_0}^{t} [\Delta T_{HW}(t') + \Delta T_{SW}(t')]dt'}. \tag{15}$$

Figure 8a, b show the estimated relative errors of the thermal conductivity and the specific heat capacity when these properties are simultaneously estimated. The figures labeled (I) and (II) refer to the use of the

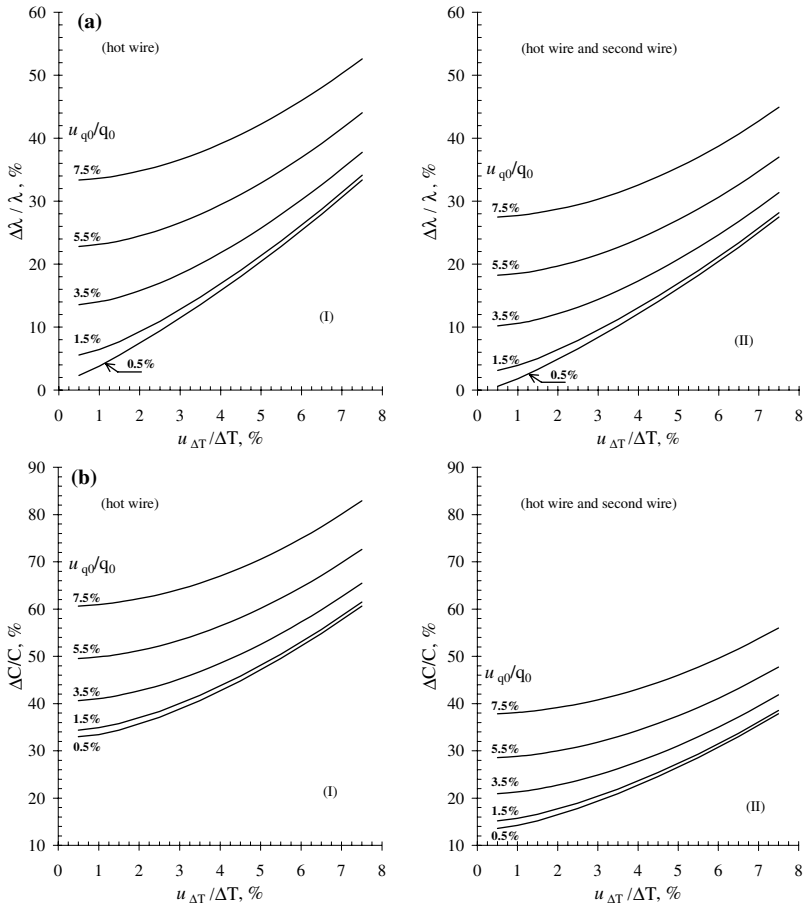

Fig. 8. Extended relative uncertainty of (a) the thermal conductivity and (b) the specific heat capacity per unit volume vs. the relative uncertainty of the temperature rise, for a few different relative uncertainties on the constant heat flux per unit length.

single and two-wire techniques, respectively. When the second wire is also applied, with the same measurement uncertainties, the estimated relative error of the properties decreases with respect to the use of only the hot wire for both the thermal conductivity and specific heat capacity. With the second wire, when its position uncertainty is not greater than 0.5%, the reliability of the estimated properties increases on average by 5% for the thermal conductivity and by 22% for the specific heat capacity. The use of the second wire is useful only when the uncertainty of its relative position is better than 5%.

5. CONCLUSIONS

A two-wire analysis, based on the classical analytical solution for the line-source method, was proposed with a constant heat flux generated from the hot wire. Using a dimensionless approach, the influences of several uncertainties and bias introduced by the model were considered to estimate their influence on the determination of the fluid properties. The results of this analysis can be summarized as follows:

- the presence of the second wire does not significantly perturb the thermal field in the fluid when its position is not close to the hot wire ($\eta > 40$);
- when a large diameter of the hot wire is used, it is possible to determine a lower limit of the Fourier number above which the effects of these finite properties are negligible; this limiting value of the Fourier number depends on the examined fluid;
- the hot wire length and radius, the position of the potential leads, and the maximum experimental duration, are related. In order to limit the axial conduction along the wire, the convection and the radiation effects, by choosing, for example, the hot-wire radius, all the other previously mentioned quantities can be determined. In this case the line-source solution could be used without correction;
- the use of two wires instead of one could improve the reliability of the simultaneously estimated properties;
- the second wire is useful to improve the properties estimation of liquids only when its relative position uncertainty is better than 5%.

The extended uncertainties of the estimated properties improve on average by 5% for the thermal conductivity and by 22% for the specific heat capacity when two wires are used instead of only the hot wire. To verify the reliability of the two-wire technique, appropriate experimental tests will be carried out.

ACKNOWLEDGMENT

The authors would like to thank Dr F. Righini for his useful suggestions.

NOMENCLATURE

C	specific heat capacity per unit of volume of the fluid
D	dimensionless radiation coefficient, $Kn^2\sigma T_0^3 r_{\mathrm{HW}}^2/\lambda$
$Ei(-)$	exponential integral
g	acceleration of gravity
G	Euler constant
$J_k(-)$	Bessel function of the first kind and order k
K	average absorption coefficient
n	refractive index
q	heat rate per unit time and per unit length generated from the hot wire
r	generic radial position
r_{HW}	hot-wire radius
r_{SW}	second-wire radial position
t	time
T_0	initial cell temperature
T_{ref}	reference temperature for the estimated properties
u	uncertainty
$Y_k(-)$	Bessel function of the second kind and order k
z	convection penetration distance from the leading edge

Greek Symbols

β	isobaric thermal expansion coefficient
γ	ratio between the length and the radius of the hot wire
δ	ratio between the specific heat capacity of the fluid and the specific heat capacity of the wire
ΔT	measured temperature rise
$\Delta T'$	line-source solution temperature rise
$\Delta\vartheta$	dimensionless temperature deviation, $\vartheta - \vartheta'$; or dimensionless temperature deviation due to the influence of the second wire
ε	ratio between the radius of the second wire and the hot wire
ζ	dimensionless convection penetration distance, $z\lambda/(g\beta q_0 t^2)$
η	dimensionless radial position from the hot wire axis, referring to the second-wire radius, r/r_{SW}
ϑ	dimensionless temperature rise, $\lambda\Delta T/q_0$

ϑ' dimensionless temperature rise with line-source hypothesis, $\lambda \Delta T'/q_0$
λ thermal conductivity of the fluid
Λ ratio between the estimated properties λ' and their correct value λ
μ ratio between the thermal conductivity of the wire to that of the fluid
ν integration variable
ξ dimensionless radial position from the hot wire axis, referring to the hot-wire radius, r/r_{HW}
σ Stefan-Boltzmann constant
τ Fourier number referring to the hot-wire radius, $\lambda t/(Cr_{\mathrm{HW}}^2)$
τ^* Fourier number referring to the second-wire radius, $\lambda t/(Cr_{\mathrm{SW}}^2)$
φ dimensionless heat generation, ε^2/π
χ ratio between the estimated properties C' and their correct value C
ψ relative variation of the heat rate per unit time and per unit length generated from the hot wire

REFERENCES

1. H. S. Carlslaw and J. C. Jaeger, *Conduction of Heat in Solids* (Oxford University Press, London, 1959), p. 261.
2. J. W. Haarman, *Physica* **52A**:605 (1971).
3. J. J. De Groot, J. Kestin, and H. Sookiazian, *Physica* **75**:454 (1974).
4. J. J. Healy, J. J. de Groot, and J. Kestin, *Physica* **82C**:392 (1976).
5. C. A. Nieto de Castro, J. C. G. Calado, W. A. Wakeham, and M. Dix, *J. Phys. E: Sci. Instrum.* **9**:1073 (1976).
6. J. Menashe and W. A. Wakeham, *Int. J. Heat Mass Transfer* **25**:661 (1982).
7. J. J. De Groot, J. Kestin, H. Sookiazian, and W. A. Wakeham, *Physica* **92A**:117 (1978).
8. A. A. Clifford, J. Kestin, and W. A. Wakeham, *Physica* **97A**:287 (1979).
9. J. Kestin, R. Paul, A. A. Clifford, and W. A. Wakeham, *Physica* **100A**:370 (1980).
10. E. N. Haran and W. A. Wakeham, *J. Phys. E: Sci. Instrum.* **15**:839 (1982).
11. R. A. Perkins, D. G. Friend, H. M. Roder, and C. A. Nieto de Castro, *Int. J. Thermophys.* **12**:965 (1991).
12. M. Hoshi, T. Omotani, and A. Nagashima, *Rev. Sci. Instrum.* **52**:755 (1981).
13. Y. Nagasaka and A. Nagashima, *Rev. Sci. Instrum.* **52**:229 (1981).
14. A. Saito, K. Matsumoto, and Y. Utaka, *JSME Int. J.* **30**:1935 (1987).
15. S. Takizawa, H. Murata, and A. Nagashima, *Bull. JSME* **21**:273 (1978).
16. R. A. Perkins, S. S. Mohammadi, R. McAllister, M. S. Graboski, and E. Dendy Sloan, *J. Phys. E: Sci. Instrum.* **14**:1279 (1981).
17. N. Kitazawa and A. Nagashima, *Bull. JSME* **24**:374 (1981).
18. U. Gross, Y. W. Song, and E. Hahne, *Int. J. Thermophys.* **13**:957 (1992).
19. R. Greger and H. J. Rath, *Int. J. Heat Mass Transfer* **38**:1105 (1995).
20. W. N. Trump and H. W. Luebke, *Rev. Sci. Instrum.* **48**:47 (1977).

21. Y. H. Julia, J. F. Renaud, D. J. Ferrand, and P. F. Malbrunot, *Rev. Sci. Instrum*. **48**:1654 (1977).
22. Y. Nagasaka and A. Nagashima, *J. Phys. E: Sci. Instrum*. **14**:1435 (1981).
23. N. Kawaguchi, Y. Nagasaka, and A. Nagashima, *Rev. Sci. Instrum*. **56**:1788 (1985).
24. E. Hahne, U. Gross, and Y. M. Song, *Int. J. Thermophys*. **10**:687 (1989).
25. E. Takegoshi, S. Imura, Y. Horasawa, and T. Takenaka, *Bull. JSME* **25**:395 (1982).
26. P. Anderson and G. Backstrom, *Rev. Sci. Instrum*. **47**:205 (1976).
27. W. R. Davis, in *Compendium of Thermophysical Property Measurement Methods: Vol. 1., Survey of Measurement Techniques,* K. D. Maglic, A. Cezairliyan, and V. E. Peletsky, eds. (Plenum Press, New York, 1984), pp. 231–254.
28. P. Prelovsec and B. Uran, *J. Phys. E: Sci. Instrum*. **17**:674 (1984).
29. M. Take-Uchi and M. Suzuki, *Bull. JSME* **27**:2449 (1984).
30. C. Glatzmaier Greg and W. F. Ramirez, *Rev. Sci. Instrum*. **56**:1394 (1985).
31. M. M. Sorour, M. M. Saleh, and R. A. Mahmoud, *Int. Comm. Heat Mass Transfer* **17**:189 (1990).
32. R. Larsson and O. Andersson, *J. Eng. Tribol*. **214**:337 (2000).
33. A. E. Wechsler, in *Compendium of Thermophysical Property Measurement Methods: Vol. 2., Recommended Measurement Technique and Practices,* K. D. Magli, A. Cezairliyan, and V. E. Peletsky, eds. (Plenum Press, New York, 1992), Chap. 6.
34. H. S. Carlslaw and J. C. Jaeger, *Conduction of Heat in Solids* (Oxford University Press, London, 1959), pp. 341–342.
35. W. H. Press, S. A. Teukolsky, W. T. Vetterling, and B. P. Flannery, *Numerical Recipes in Fortran* 77, 2nd Ed. (Cambridge University Press, New York, 1992).
36. M. Abramowitz and I. A. Stegun, *Handbook of Mathematical Functions* (Dover, New York, 1972), pp. 358–389.
37. J. H. Blackwell, J. *Appl. Phys*. **25**:137 (1954).
38. J. H. Blackwell, *Can. J. Phys*. **34**:412 (1956).
39. R. J. Goldstein and D. G. Briggs, *J. Heat Transfer Trans. ASME C* **86**:490 (1964).
40. C. A. Nieto de Castro, R. A. Perkins, and H. M. Roder, *Int. J. Thermophys*. **12**:985 (1991).
41. L. Sun, J. E. S. Venart, and R. C. Prasad, *Int. J. Thermophys*. **23**:1487 (2002).
42. V. Giaretto and M. F. Torchio, *High Temp.-High Press*. **31**:643 (1999).
43. V. Giaretto, E. Miraldi, and G. Ruscica, *High Temp.-High Press*. **27/28**:191 (1995/96).
44. J. V. Beck and K. J. Arnold, *Parameter Estimation in Engineering and Science* (John Wiley, New York, 1977), pp. 259–269.